INTERNATIONAL JOURNAL FOR NUMERICAL METHODS IN FLUIDS, VOL. 11, 893–906 (1990)

FINITE ELEMENT METHODS FOR ONE-DIMENSIONAL COMBUSTION PROBLEMS

J. I. RAMOS

Department of Mechanical Engineering, Carnegie-Mellon University, Pittsburgh, PA 15213, U.S.A.

SUMMARY

Three adaptive finite element methods based on equidistribution, elliptic grid generation and hybrid techniques are used to study a system of reaction–diffusion equations. It is shown that these techniques must employ sub-equidistributing meshes in order to avoid ill-conditioned matrices and ensure the convergence of the Newton method. It is also shown that elliptic grid generation methods require much longer computer times than hybrid and static rezoning procedures. The paper also includes characteristic, Petrov–Galerkin and flux-corrected transport algorithms which are used to study a linear convection–reaction–diffusion equation that has an analytical solution. The flux-corrected transport technique yields monotonic solutions in good agreement with the analytical solution, whereas the Petrov–Galerkin method with quadratic upstream-weighted functions results in very diffused temperature profiles. The characteristic finite element method which uses a Lagrangian–Eulerian formulation overpredicts the flame front location and exhibits overshoots and undershoots near the temperature discontinuity. These overshoots and undershoots are due to the interpolation of the results of the Lagrangian operator onto the fixed Eulerian grid used to solve the reaction–diffusion operator, and indicate that characteristic finite element methods are not able to eliminate numerical diffusion entirely.

KEY WORDS Adaptive Characteristic Flux-corrected Transport Petrov–Galerkin Finite Elements

INTRODUCTION

The objective of this paper is twofold. First, three adaptive finite element methods are used to study a system of one-dimensional reaction–diffusion equations. The adaptive finite elements employed in this study are based on a variational formulation[1] which accounts for grid smoothness and grid equidistribution by means of two parameters. It is shown that if the smoothness parameter is set to zero, the minimization of the functional yields an equidistributing mesh, whereas if the two parameters are different from zero, the minimization yields a non-linear elliptic equation for the grid motion. A hybrid technique which combines elliptic grid generation and mesh equidistribution techniques is also presented.

The second objective of this paper is to assess the accuracy of characteristic, Petrov–Galerkin and flux-corrected transport finite element methods in the solution of a one-dimensional linear convection–reaction–diffusion equation which has an analytical solution.

Adaptive grid generation techniques may be classified into three broad categories: static rezoning, moving and hybrid methods.[2] In static rezoning methods the grid nodes may remain fixed for intervals of time, whereas the grid motion and the integration of the partial differential equations are fully coupled in moving or dynamic methods. Hybrid techniques are intermediate between static rezoning and moving methods.[3]

0271–2091/90/140893–14$07.00

Received July 1989

The grid adaptation in static rezoning techniques may be based on the equidistribution of a positive weight function, finite element residuals, solution gradients, *a priori* and *a posteriori* error estimates, variational formulations, etc.[2,4,5] Moving or dynamic adaptive techniques may be based on mesh equidistribution,[6] transformation[7] and variational[1,8,9] principles, moving finite element methods with and without error control,[10,11] solution of partial differential equations, etc.[2,3,5]

In this paper the variational formulation of Brackbill and Saltzman[1] is used to study a system of two reaction–diffusion equations which model one-dimensional flame propagation.[12] It is shown that such a variational formulation results in equidistribution and elliptic grid generation techniques by appropriate choices of the parameters which govern the grid smoothness and the grid equidistribution. Such a formulation has been previously used by the author to study the spherical ignition of homogeneous gaseous mixtures[13] and is presented in the next section.

The third section of this paper deals with the solution of a linear convection–reaction–diffusion equation which has an analytical solution and which is solved by means of Petrov–Galerkin, characteristic and flux-corrected transport finite element methods for finite and infinite Peclet numbers.

Petrov–Galerkin finite element methods use different subspaces for the trial and test functions and lead to upwind finite element approximations with non-symmetric or non-centred Galerkin equations.[14] The test or weight functions bias the upstream influence relative to the flow direction in convection-dominated flows. The weight functions generally contain a parameter which must be chosen so as to optimize the numerical results. With upstream-weighted test functions the solution of convection-dominated flows does not exhibit oscillations, but is smoothed out because of the numerical dissipation terms introduced by upwinding. Numerical damping is particularly severe if the flow has steep gradients. Christie *et al.*[15] and Hughes[16] have determined the conditions under which the solution of the Petrov–Galerkin finite element methods coincides with the exact one for simple convection–diffusion equations, and the conditions for which the solution of the finite element method is fourth-order accurate in space. Hughes[17] has recently presented a review of streamline upwind Petrov–Galerkin methods (SUPG), while Ramos[2] has reviewed different upwinding strategies for convection–diffusion–reaction equations.

Characteristic finite element techniques use operator-splitting algorithms to reduce a system of convection–diffusion–reaction equations to a sequence of convection and reaction–diffusion operators.[18] The convection operator can be solved by means of the method of characteristics, i.e. using a Lagrangian approach which eliminates the numerical dissipation that would be introduced if the convection operator were solved in a fixed grid. The solution of the convection operator can then be interpolated onto a fixed Eulerian grid where the reaction–diffusion operator is solved. Since both the method of characteristics and fixed grids are employed in the calculations, characteristic finite element methods may be also referred to as Lagrangian–Eulerian formulations.

Since the method of characteristics is used to solve the convection operator, the numerical dissipation which will occur in convection-dominated flows when fixed grids are used to solve that operator is eliminated. However, some numerical diffusion errors are still present owing to the interpolation of the results of the method of characteristics onto a fixed grid. It will be shown in this paper that such interpolation may result in overshoots and undershoots when steep flow gradients exist.

A third method for reducing numerical dissipation errors in convection-dominated flows is the flux-corrected transport (FCT) algorithm.[19,20] This algorithm is monotone and preserves positivity, and has been applied to the Euler and Navier–Stokes equations.[21,22]

In this paper an FCT finite element method is used to solve a linear convection–diffusion–reaction equation, and its results are compared with the analytical solution and with those of characteristic and Petrov–Galerkin finite element methods for several values of the Peclet number.

REACTION–DIFFUSION EQUATIONS

Consider the Dwyer–Sanders model of flame propagation for homogeneous gaseous mixtures confined between two infinite parallel planar walls. The equations governing the model can be written as[12]

$$Y_t = Y_{xx} - YR(T), \qquad T_t = T_{xx} + YR(T), \qquad 0<x<1, \quad t>0, \tag{1}$$

$$Y(x, 0) = 1, \qquad T(x, 0) = 0{\cdot}2, \tag{2}$$

$$Y_x(0, t) = T_x(0, t) = 0, \tag{3}$$

$$Y_x(1, t) = 0, \qquad T(1, t) = f(t), \tag{4}$$

where

$$R(T) = 3{\cdot}52 \times 10^{-6} \exp(-4/T), \tag{5}$$

$$f(t) = \begin{cases} 0{\cdot}2 + t/0{\cdot}0002, & 0<t<0{\cdot}0002, \\ 1{\cdot}2, & t \geqslant 0{\cdot}0002. \end{cases} \tag{6}$$

All the variables are dimensionless: t is time, x is the spatial co-ordinate, Y is the species mass fraction, T is the temperature, the subscripts denote differentiation and R is the reaction rate.

Equation (1) can be written as

$$\mathbf{U}_t = \mathbf{F}(\mathbf{U}), \tag{7}$$

where

$$\mathbf{U} = (Y, T)^{\mathrm{T}}, \qquad \mathbf{F} = [Y_{xx} - YR(T), \qquad T_{xx} + YR(T)]^{\mathrm{T}}; \tag{8}$$

the superscript T denotes transpose.

Equation (7) was solved by means of a Galerkin finite element method which uses linear basis functions[14] and by means of three adaptive numerical methods based on the variational formulation proposed by Brackbill and Saltzman[1] as follows.

We first introduce the mapping

$$(x, t) \rightarrow (\eta, \tau), \tag{9}$$

where

$$\tau = t, \qquad \eta = \int_0^x w(y, t)\,\mathrm{d}y \Big/ \int_0^1 w(y, t)\,\mathrm{d}y; \tag{10}$$

$w(x, t)$ is a weighting function, which in our case was taken as the arc length of the temperature profile, i.e.

$$w = \left[1 + \left(\frac{\partial T}{\partial x}\right)^2\right]^{1/2}. \tag{11}$$

We now introduce the functional[1]

$$I = \lambda_s \int_0^1 \left(\frac{\partial \eta}{\partial x}\right)^2 dx + \lambda_v \int_0^1 w(x,t) J\, dx, \tag{12}$$

where λ_s and λ_v are two parameters and

$$J = \frac{\partial(x,t)}{\partial(\eta,\tau)} = x_\eta \tag{13}$$

is the Jacobian of the transformation defined by equation (9).

The first and second integrals in equation (12) are related to grid smoothness and grid equidistribution respectively.

Minimization of equation (12) yields the Euler–Lagrange equation

$$\lambda_s x_{\eta\eta} + \lambda_v x_\eta^3 (w x_{\eta\eta} + x_\eta^2 w_x) = 0, \tag{14}$$

which is a non-linear elliptic equation whose solution yields $x(\eta,\tau)$. Note that if $\lambda_v = 0$, equation (14) yields $x_\eta = C(\tau)$, i.e. the grid spacing in the x-co-ordinate is proportional to that in the η-co-ordinate. However, if $\lambda_s = 0$, equation (14) can be integrated to yield the equidistribution equation

$$w x_\eta = C(\tau), \tag{15}$$

where $C(\tau)$ denotes a function of τ.

For an equally spaced grid in the η-co-ordinate, equation (15) implies that the grid spacing in the x-co-ordinate is inversely proportional to w, i.e. the grid points will be concentrated where w is largest; that is, where the temperature gradient is largest.

In the next subsections, three adaptive techniques based on equation (14) are described.

Equidistribution method

In this method the grid is distributed according to equation (15), i.e. $\lambda_s = 0$, which can be used to calculate the mesh spacing in the x-co-ordinate as follows. Assume that the mesh is equally spaced in the η-co-ordinate with $NP = NE + 1$ grid points and NE finite elements. Then equation (15) can be written as

$$\frac{j-1}{NE} = \int_0^{x_j} w\, dx \Big/ \int_0^1 w\, dx, \quad i = 2, 3, \ldots, NE, \tag{16}$$

with $x_1 = 0$ and $x_{NP} = 1$.

Equation (7) was solved by means of a linear Galerkin finite element method, and its solution was used to calculate the weighting function w (equation (11)). Once w is known, the location x_j of the jth grid point can be calculated from equation (16). However, the equidistribution technique defined by equation (15) does not ensure grid smoothness and, as a consequence, the sizes of adjacent finite elements may be quite different. This may result in numerical difficulties, e.g. slow convergence and ill-conditioned matrices, and numerical errors when solving the finite element discretization of equation (7).

In order to ensure grid smoothness and avoid adjacent finite elements of quite different sizes, the following sub-equidistribution method was employed:[2,3]

$$k^{-1} \leqslant h_{i+1}/h_i \leqslant k, \tag{17}$$

where $k \geqslant 1$ and the element size or grid spacing is

$$h_i = x_i - x_{i-1}, \quad i = 2, 3, \ldots, NP. \tag{18}$$

Equation (17) imposes lower and upper bounds on the ratio of the sizes of adjacent elements.

Equations (7), (16) and (17) were used in the present study as follows. The finite element discretization of equation (7) was first obtained and used to calculate x_j from equation (16). When equation (17) was violated, grid points were added/deleted and the new grid was used to solve equation (16). This procedure was repeated as many times as necessary at each time step, and may be referred to as a static rezoning technique because the grid addition/deletion is effected once the solution is known.

In the next subsection a moving technique based on equation (14) is described.

Elliptic grid generation

Equation (14) determines the location of the grid points in the x-co-ordinate. This equation is elliptic, corresponds to a two-point non-linear boundary value problem with $x(0, \tau) = 0$ and $x(1, \tau) = 1$, and can be solved at each time step coupled with the solution of equation (7) which can be written as

$$\mathbf{U}_\tau = \mathbf{F}(\mathbf{U}) + \mathbf{U}_x x_\tau, \tag{19}$$

where the grid velocity x_τ can be calculated from equation (10) as

$$x_\tau = -\eta_t x_\eta = -\eta_t/\eta_x, \qquad \eta_x = w \Big/ \int_0^1 w \, dx, \tag{20}$$

and, η_t can be calculated from equation (10).

The finite element discretizations of equation (14) with $\lambda_s = \lambda_v = 1$ and of equation (19) use the linear Galerkin finite element method for both x and $\mathbf{U}$, i.e.

$$\mathbf{U} = \sum_{i=1}^{NP} \mathbf{U}_i(\tau)\phi_i(\xi), \qquad x = \sum_{i=1}^{NP} x_i(\tau)\phi_i(\xi), \tag{21}$$

where ξ is the local co-ordinate in each element, i.e. $\xi = NE(\eta - \eta_{i-1})$ for $\eta_{i-1} \leqslant \xi \leqslant \eta_i$, ϕ is a linear basis function and $\mathbf{U}_i$ and x_i denote the nodal amplitudes of the finite element approximation to $\mathbf{U}$ and x, respectively.

The Galerkin finite element discretizations of equations (14) and (19) yield a system of algebraic equations for x_i and a system of ordinary differential equations for $\mathbf{U}_i$; the first-order time derivatives were discretized by means of first-order accurate backward difference formulae and the resulting system of non-linear algebraic equations was solved by means of a damped Newton method.

However, the finite element discretizations of equations (14) and (19) did not converge when a small fixed number of grid points was used in the calculations, and, in some cases, numerical instabilities were also observed. The reason for the lack of convergence and for instabilities was ill-conditioned and stiff matrices, i.e. the Jacobian of the non-linear algebraic equations was such that the ratio of its largest to its smallest eigenvalue was, in absolute value, much larger than one. This was found to be a consequence of the very disparate finite element sizes which result when a fixed number of grid points is used in the calculations.

In order to ensure the convergence of the Newton method and avoid ill-conditioned systems, the sub-equidistribution technique defined by equation (17) was used in the calculations as

follows. Equations (14) and (19) were first solved. If after a certain number (50) of iterations the Newton method did not converge, or if it converged but violated equation (17), grid points were added or deleted. Equations (14) and (19) were then solved in the new grid and the procedure was repeated until convergence was achieved and equation (17) was satisfied.

Owing to the iterative character of the Newton method and the sub-equidistribution technique employed in the calculations, the elliptic grid generation method presented in this subsection required much longer computational times than the static rezoning procedure described in the previous subsection.

The main advantage of the elliptic grid generation method is that the grid motion (equation (14)) and the solution of the reaction–diffusion equations (equation (19)) are coupled at each time step; therefore the grid adaptively follows the largest temperature gradients. However, the grid motion may result in finite element of disparate sizes, ill-conditioned matrices and non-convergence of the Newton method if a fixed number of finite elements is used in the calculations. These problems can be reduced somewhat by using a sub-equidistribution technique to ensure grid smoothness.

Note that equation (14) contains a smoothness parameter λ_s; however, calculations with a fixed number of grid points and $0{\cdot}5 \leqslant \lambda_s \leqslant 10$ indicated that sub-equidistribution was still necessary in order to achieve convergence and/or accurate results.

In the next subsection we develop a hybrid adaptive method which uses the grid distribution provided by equation (14) but decouples the solution of equations (14) and (19).

Hybrid method

In static rezoning techniques the grid points may remain fixed for intervals of time, whereas in elliptic grid generation methods the solution of the partial differential equations and the grid motion are fully coupled at each time step. Hybrid methods are intermediate between static and fully dynamic adaptive procedures.

In this subsection we describe a hybrid method which combines the advantages of the equidistribution and elliptic grid generation techniques presented in the previous subsections. For the sake of convenience our discussion will be limited for calculations starting at $t=0$. At $t=0$ we know the initial values of $\mathbf{U}$ and w; therefore equation (14) can be solved to obtain a grid. This grid must satisfy the sub-equidistribution equation (17); wherever equation (17) is violated, grid points are inserted or deleted and equation (14) is solved in the new grid. This procedure is repeated as many times as necessary until equation (17) is satisfied. The grid thus determined at $t=0$ is used to solve equation (7) and advance the solution from $t=0$ to $t=\Delta t$, where Δt is the time step. The solution at Δt is then used to calculate a new grid at this time level by solving equation (14) subject to equation (17).

From the previous discussion it can be concluded that in hybrid methods the nodal locations lag the solution of the partial differential equations, i.e. the grid motion and the solution of the governing equations are not coupled at each time step; rather, the solution at the previous time is used to calculate the new nodal locations.

This lag may result in severe inaccuracies if the flame speed and/or the time step are large, but can be reduced by reducing the time step. Furthermore, since the nodes occupy different positions at different times, interpolation is necessary. This interpolation must be performed so as to preserve the monotonicity and positivity of the solution and conservation of mass (species) and energy. Otherwise, oscillatory solutions may be obtained and/or the interpolated solution may violate mass and energy conservation. In the calculations presented here we have used cubic splines for the interpolation.

Presentation of results

Figures 1 and 2 show the temperature and species mass fraction profiles at selected times, while the locations of some of the grid points used in the calculations are presented in Figure 3. Figures 1–3 were obtained with the elliptic grid generation technique and the number of grid points varied from 15 to 25. Verwer *et al.*[3] solved equation (7) by means of a predictor–corrector hybrid finite difference method and used between 10 and 17 grid points, a variable time step and a weighting function proportional to the square root of the absolute value of the second derivative of the temperature.

The predictor step of the method used by Verwer *et al.*[3] is identical to the hybrid method described in this paper. Their corrector step uses the results of our hybrid method to calculate the new grid at $t=\Delta t$, which is then employed to solve equation (19).

The results of the static rezoning and hybrid methods are almost identical to those presented in Figures 1–3; however, the computational times are vastly different. The static rezoning, hybrid and elliptic grid generation methods used the same time step and required 41, 69 and 218 min of CPU

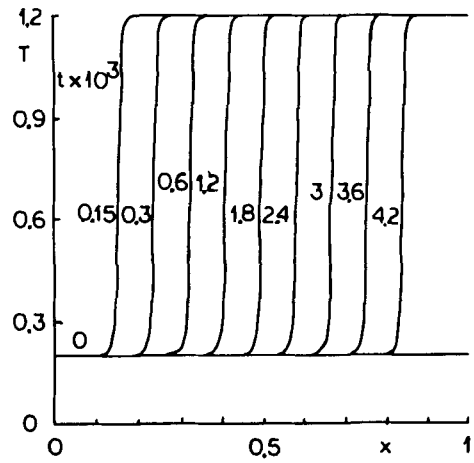

Figure 1. Temperature profiles

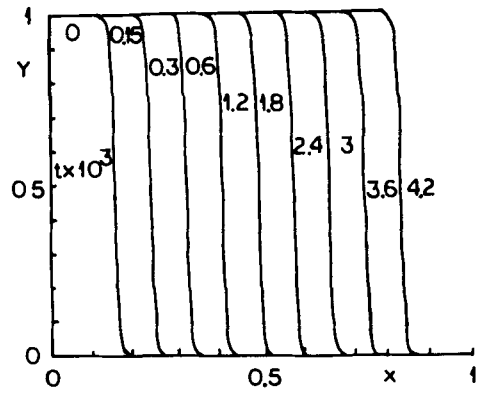

Figure 2. Mass fraction profiles

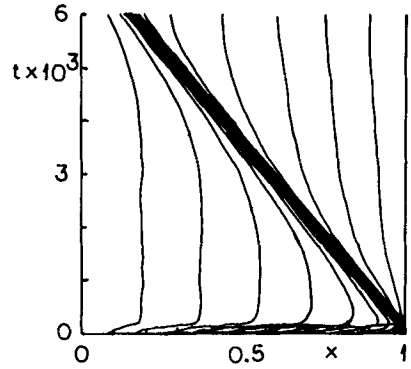

Figure 3. Grid point locations

time on a VAX 11/780 computer. The differences in computer times are due to the solution of the elliptic grid generation method and to the non-linear coupling between the grid motion and the solution of the partial differential equations in the elliptic grid generation procedure.

CONVECTION–REACTION–DIFFUSION EQUATIONS

In this section we consider the following non-dimensional linear convection–reaction–diffusion equation:[2,24]

$$T_t + T_x = \frac{1}{Pe} T_{xx} - \beta T, \quad 0 < x < \infty, \quad t > 0, \tag{22}$$

subject

$$T(x, 0) = \frac{\partial T}{\partial x}(\infty, t) = 0, \tag{23}$$

$$T(0, t) = \exp(-\beta t), \tag{24}$$

where Pe is the Peclet number and β is a constant.

Equation (22) is a model equation which, for $Pe = \infty$, has the following analytical solution obtainable by means of the Laplace transform:[24]

$$T(x, t) = e^{-\beta t} H(t - x), \tag{25}$$

where $H(\eta)$ is the Heaviside step function, i.e. $H = 1$ for $\eta > 0$ and $H = 0$ for $\eta < 0$.

Equation (22) was solved by means of the finite element methods described in the next subsections.

Characteristic finite element method

Equation (22) can be written in operator-splitting form as the following sequence of convection and reaction–diffusion operators:

$$L_c: \quad T_t + T_x = 0, \tag{26}$$

$$L_{RD}: \quad T_t = \frac{1}{Pe} T_{xx} - \beta T. \tag{27}$$

The solution of equation (26) can be obtained exactly by means of the method of characteristics to yield $T=$constant along the characteristic line

$$dx/dt = 1. \tag{28}$$

Equation (28) can be integrated to yield

$$\bar{x} = x^n + \Delta\bar{t}, \tag{29}$$

where $\Delta\bar{t}$ denotes the time step used to solve the convection operator, x^n denotes the co-ordinate at t^n and $\bar{x}$ denotes the co-ordinate which results from the convection operator. The value of $\bar{x}$ does not, in general, coincide with the location of the fixed grid points used to solve the reaction–diffusion operator. Therefore the temperature value from the convection operator must be interpolated onto the fixed grid of the reaction–diffusion operator which was solved by means of a Galerkin linear finite element method.

Since equation (26) and (27) are based on the method of characteristics and fixed grids for the reaction–diffusion operator, the resulting technique may be referred to as characteristic–Eulerian or Lagrangian–Eulerian method. Note that the advantage of characteristic finite element methods is the elimination of the convection term. However, numerical diffusion cannot be eliminated entirely because of the interpolation required to project the results of the convection operator onto the Eulerian grid of the reaction–diffusion operator.

Petrov–Galerkin finite element method

Equation (22) was also solved by means of a Petrov–Galerkin finite element method which introduces upwinding by biasing upstream influence relative to the flow direction.

We have used trial functions ϕ_i which are piecewise linear, whereas the test or weight functions can be written as[14, 15] (Figure 4)

$$w_1 = \phi_1 + \alpha F_1(\xi), \qquad w_2 = \phi_2 - \alpha F_1(\xi), \tag{30}$$

$$F(\xi) = -3(\xi^2 - \xi), \qquad \xi = (x - x_i)/(x_{i+1} - x_i), \qquad x_i \leqslant x \leqslant x_{i+1}, \tag{31}$$

and the value of α was selected so as to avoid oscillatory solutions.

With the upstream-weighted functions given by equation (30) and a proper choice of α, the solution of equation (22) does not exhibit oscillations but is smoothed out because of the numerical dissipation introduced by upwinding. Damping is particularly severe when the flow has steep gradients, e.g. for $Pe = \infty$.

FCT finite element method

Flux-corrected transport (FCT) techniques are monotone positivity-preserving methods which reduce the amount of numerical dissipation introduced by Petrov–Galerkin finite element methods and involve the following steps:[19, 20] (1) calculate the convection fluxes by a low-order

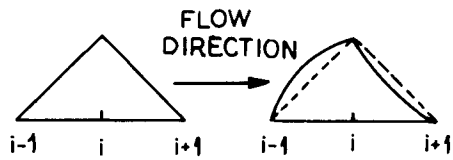

Figure 4. Upstream weight functions

monotone algorithm; (2) calculate the fluxes by a high-order method: (3) calculate the antidiffusion flux as the difference between the fluxes computed in steps 1 and 2; (4) calculate the low-order transported and diffused solution; (5) bound the magnitude of the antidiffusion flux so that the solution of step 6 is free of overshoots and undershoots; (6) use the limited antidiffusion fluxes to obtain a new solution.

In the calculations presented in this paper, equation (22) was operator-split as in equations (26) and (27). Equation (27) was solved by means of a Galerkin linear finite element method, while equation (26) was solved by means of the FCT technique as follows. Equation (26) can be written using Taylor series expansions as

$$T^* = T^n - \Delta t\left(\frac{\partial T}{\partial x}\right)^n + \frac{\Delta t^2}{2}\left(\frac{\partial^2 T}{\partial x^2}\right)^n + O(\Delta t^3), \tag{32}$$

where T^* denotes the solution of the convection operator. Applying linear (Taylor–Galerkin) finite element methods, equation (32) can be written as[21]

$$\mathbf{M}\Delta\mathbf{T}^* = \mathbf{R}, \qquad \Delta\mathbf{T}^* = \mathbf{T}^* - \mathbf{T}^n, \tag{33}$$

where $\mathbf{M}$ is the mass matrix, $\mathbf{T}^*$ is the vector of nodal amplitudes and $\mathbf{R}$ denotes the corresponding right-hand-side terms.

A low-order solution of equation (33) can be obtained by solving the equation

$$\mathbf{M}_L\Delta\mathbf{T}^1 = \mathbf{R} + \mathbf{A}, \tag{34}$$

where $\mathbf{M}_L$ is the lumped mass matrix, $\mathbf{A}$ is a vector of artificial viscosity and $\mathbf{T}^1$ denotes the low-order diffused solution. The vector $\mathbf{A}$ can be written as

$$\mathbf{A} = c_d(\mathbf{M} - \mathbf{M}_L)\mathbf{T}^n, \tag{35}$$

where c_d is a diffusion coefficient.

The antidiffusive step can be written as the difference between equation (33) and (35), i.e.

$$\mathbf{M}_L(\Delta\mathbf{T}^* - \Delta\mathbf{T}^1) = (\mathbf{M}_L - \mathbf{M})\Delta\mathbf{T}^* - \mathbf{A}, \tag{36}$$

which can be expressed as

$$\Delta\mathbf{T}^* - \Delta\mathbf{T}^1 = \mathbf{M}_L^{-1}(\mathbf{M}_L - \mathbf{M})(\Delta\mathbf{T}^* + c_d\mathbf{T}^n). \tag{37}$$

The right-hand-side of equation (36) has to be limited so as to avoid overshoots and undershoots in equation (37).

For all the finite element methods presented in this section, the semi-finite domain $0 \leqslant x < \infty$ was truncated to $0 \leqslant x < L$, and the computations were performed up to a time such that the temperature profiles are not affected by the value of L.

Presentation of results

Figures 5–7 show the value of T as a function of x at $t = 1$, and for $\beta = 1$, $L = 2$ and $Pe = \infty$, 0·25 and 0·01 respectively. In these figures A, C-FEM, P–G and FCT denote the analytical solution and the characteristic, Petrov–Galerkin and flux-corrected transport finite element methods respectively.

Figure 5 indicates that the C-FEM yields overshoots and undershoots in the neighbourhood of the temperature discontinuity. These overshoots and undershoots are due to the interpolation of the solution of the characteristic (Lagrangian) solution of the convection operator onto the fixed (Eulerian) grid of the reaction–diffusion operator. Such an interpolation was performed with cubic

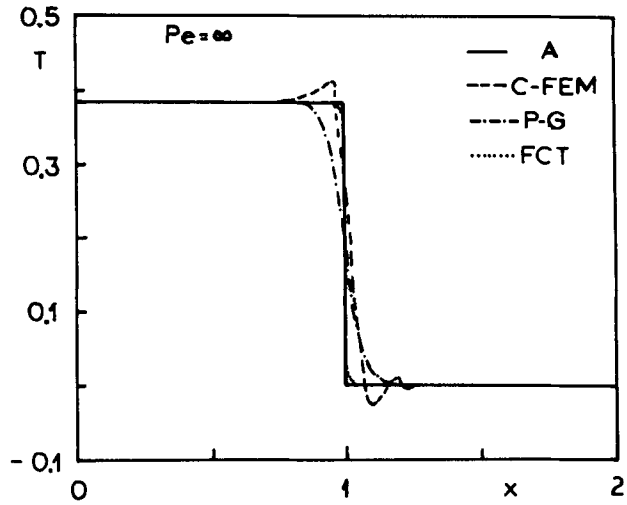

Figure 5. Temperature profiles for $Pe = \infty$

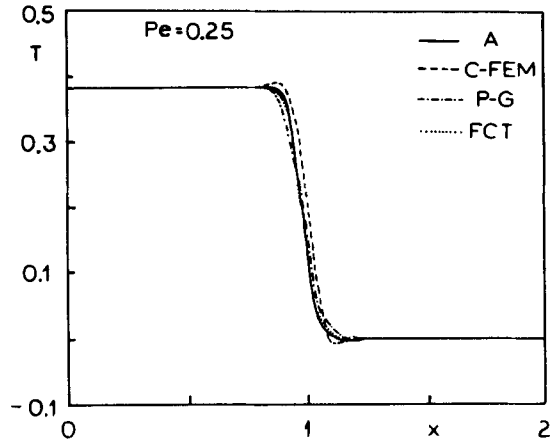

Figure 6. Temperature profiles for $Pe = 0{\cdot}25$

splines. Calculations were also performed by means of linear and quadratic interpolation and yielded similar overshoots and undershoots to those shown in Figure 5.

Figure 5 also indicates that the P–G and FCT finite element methods yield non-oscillatory solutions. However, the P–G method predicts a smoother (more diffused) temperature profile than the FCT technique. The FCT finite element method predicts a steep discontinuity except near the corners where some diffusion can be observed.

Figures 6 and 7 indicate that the smoothing of the temperature profile decreases and that the agreement between the analytical and numerical solutions improves as the Peclet number is decreased. Both Figures 6 and 7 indicate that the FCT finite element method is more accurate and predicts a steeper temperature profile than the C-FEM and P–G techniques. This higher accuracy is due to the reduction to the numerical diffusion in the antidiffusive step of the FCT algorithm.

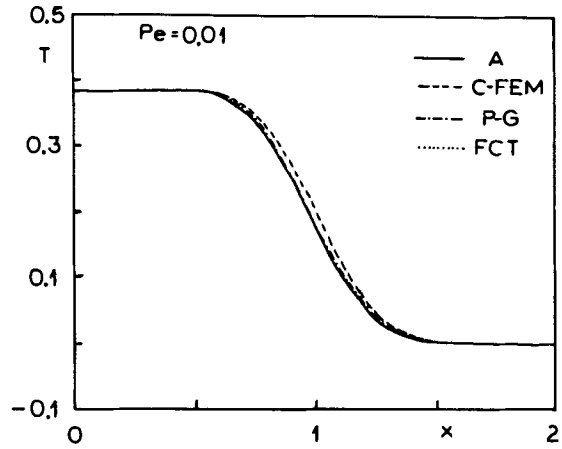

Figure 7. Temperature profiles for $Pe = 0{\cdot}01$

Figures 6 and 7 also indicate that the C-FEM method slightly overpredicts the location of the flame front and that the temperature profiles show overshoots and undershoots for $Pe = 0{\cdot}25$ but not for $Pe = 0{\cdot}01$. The overprediction of the flame front location and the overshoots and undershoots seem to be a consequence of the interpolation of the solution of the convection operator onto the Eulerian grid used to solve the reaction–diffusion operator.

CONCLUSIONS

Adaptive static rezoning, elliptic grid generation and hybrid techniques have been used to study the propagation of a one-dimensional laminar flame in Cartesian co-ordinates. The static rezoning method equidistributes the arc length of the temperature and is based on a variational formulation which does not include grid smoothness. The elliptic grid generation technique uses grid smoothness and grid equidistribution and is based on the minimization of a functional whose Euler–Lagrange equation is a two-point non-linear elliptic equation for the grid motion. The elliptic grid generation method couples the solution of the grid motion and the solution of the partial differential equations at each time step, and results in a system of non-linear algebraic equations which were solved by means of a damped Newton method.

It was found that the system of algebraic equations was, in some cases, ill-conditioned and that the Newton method did not converge unless the sizes of adjacent finite elements were bounded from above and below, i.e. it did not converge unless the grid was sub-equidistributed.

The hybrid method is intermediate between the static rezoning procedures whose grid points remain fixed for intervals of times, and elliptic grid generation techniques where the grid motion and the solution of the partial differential equations are fully coupled at each time step.

The hybrid method presented in this paper is of the predictor type, in that a known solution is used to calculate the grid at a new time level. Therefore, there is a lag between the grid motion and the solution of the partial differential equations. This lag may yield inaccurate results if the time step and/or the flame speed are large, and can be reduced by reducing the time step.

It was shown that static rezoning, elliptic grid generation and hybrid methods require mesh sub-equidistribution strategies in order to avoid ill-conditioned matrices and adjacent elements of quite different sizes. These methods resulted in almost undistinguishable results when applied to a

system of reaction–diffusion equations. However, the elliptic grid generation and hybrid methods required approximately 5·30 and 1·68 longer computer times than the static rezoning technique. These differences in computer times are due to the solution of the non-linear elliptic equation which governs the grid motion and to the mesh sub-equidistribution strategy employed in the calculations.

Characteristic, flux-corrected transport and Petrov–Galerkin finite element methods were also used to study a linear convection–diffusion–reaction equation which has an analytical solution. It was found that Petrov–Galerkin methods yield smoother temperature profiles near steep fronts than the flux-corrected transport and characteristic finite element techniques. This smoothing or numerical diffusion was caused by the use of upstream weight functions, and decreases as the Peclet number is decreased, i.e. as the flow becomes less convection-dominated.

The monotone and positivity-preserving flux-corrected transport finite element method yielded steep flame fronts in very good agreement with the analytical solution, except upstream and downstream of the temperature discontinuity for an infinite value of the Peclet number.

Both the flux-corrected transport and the characteristic finite element techniques split the convection–diffusion–reaction operator into a sequence of convection and reaction–diffusion operators. The characteristic finite element technique solves the convection operator exactly by means of the method of characteristics, but results in overshoots and undershoots at the flame front due to the interpolation of the results of the convection operator onto the fixed (Eulerian) grid used to solve the reaction–diffusion operator. The characteristic or Lagrangian–Eulerian finite element method also yields some numerical diffusion due to the interpolation. It can be concluded that very accurate solutions of convection-dominated flows can be obtained by means of flux-corrected transport finite element methods which limit the amount of antidiffusion.

ACKNOWLEDGEMENTS

This paper collects in part the oral presentation given by the author at the Seventh International Conference of Finite Element Methods in Flow Problems held at The University of Alabama in Huntsville, 3–7 April 1989. It is an extended, revised and updated version of that presentation and of the short paper published in the proceedings of that conference (Reference 13). The author is thankful to Professor T. J. Chung, general chairman of the conference, for his invitation to attend the conference and prepare this article.

REFERENCES

1. J. U. Brackbill and J. S. Saltzman, 'Adaptive zoning for singular problems in two-dimensions', *J. Comput. Phys.* **46,** 342–368 (1982).
2. J. I. Ramos, 'Finite element methods for one-dimensional flame propagation problems', in T. J. Chung (ed.), *Numerical Modeling in Combustion*, Hemisphere, Washington, DC, 1990, Chap. 3.
3. J. G. Verwer, J. G. Blom and J. M. Sanz-Serna, 'An adaptive moving grid method for one-dimensional systems of partial differential equations', *Report NM-R8804*, Centre for Mathematics and Computer Science, Amsterdam, 1988.
4. P. R. Eiseman, 'Adaptive grid generation', *Comput. Methods Appl. Mech. Eng.*, **64,** 321–376 (1987).
5. J. F. Thompson, 'A survey of dynamical adaptive grids in the numerical solution of partial differential equations', *Appl. Numer. Math.*, **1,** 3–27 (1985).
6. E. A. Dorfi and L. O'C. Drury, 'Simple adaptive grids for 1-D initial value problems', *J. Comput. Phys.*, **69,** 175–195 (1987).
7. H. A. Dwyer, 'Adaptive numerical methods for reacting flows', *Physica D*, **20,** 142–154 (1986).
8. L. R. Petzold, 'Observations of an adaptive moving grid method for one-dimensional systems of partial differential equations', *Appl. Numer. Math.*, **3,** 347–360 (1987).
9. A. C. Mueller and G. F. Carey, 'Continuously deforming finite elements', *Int. j. numer. methods eng.*, **21,** 2099–2126 (1985).
10. K. Miller and R. N. Miller, 'Moving finite elements I', *SIAM J. Numer. Anal.*, **18,** 1019–1032 (1981).

11. S. Adjerid and J. E. Flaherty, 'A moving-mesh finite element method with local refinement for parabolic partial differential equations', *Comput. Methods Appl. Mech. Eng.*, **55**, 3–26 (1986).
12. H. A. Dwyer and B. R. Sanders, 'Numerical modeling of unsteady flame propagation', *Report SAND 77-8275*, Sandia National Laboratories, Livermore, CA, 1978.
13. J. I. Ramos, 'Finite element methods for one-dimensional combustion problems', in T. J. Chung and G. R. Karr (eds.) *Finite Element Analysis in Fluids*, The University of Alabama in Huntsville Press, Huntsville, AL, pp. 283–289, 1989.
14. R. Wait and A. R. Mitchell, *Finite Element Analysis and Applications*, Wiley, New York, 1985.
15. I. Christie, D. F. Griffiths, A. R. Mitchell and O. C. Zienkiewicz, 'Finite element methods for second order differential equations with significant first derivatives', *Int. j. numer. methods eng.*, **10**, 1389–1396 (1976).
16. T. J. R. Hughes, 'A simple scheme for developing "upwind" finite element methods', *Int. j. numer. methods eng.*, **12**, 1359–1365 (1978).
17. T. J. R. Hughes, 'Recent progress in the development and understanding of SUPG methods with special relevance to the compressible Euler and Navier–Stokes equations', *Int. j. numer. methods fluids*, **7**, 1261–1275 (1987).
18. K. Fujinawa, 'A "characteristic" finite element scheme for convective-dispersive transport with non-equilibrium reaction', *Int. j. numer. methods eng.*, **23**, 1161–1178 (1986).
19. J. P. Boris and D. L. Book, 'Flux-corrected transport: I. SHASTA, A fluid transport algorithm that works', *J. Comput. Phys.*, **11**, 38–69 (1973).
20. J. P. Boris and D. L. Book, 'Flux-corrected transport: III. Minimal error FCT algorithms', *J. Comput. Phys.*, **20**, 397–431 (1976).
21. R. Löhner, K. Morgan, J. Peraire and M. Vahdati, 'Finite element flux-corrected transport (FEM-FCT) for the Euler and Navier–Stokes equations', *Int. j. numer. methods fluids*, **7**, 1093–1109 (1987).
22. J. T. Oden, T. Strouboulis and Ph. Devloo, 'Adaptive finite element methods for high-speed compressible flows', *Int. j. numer methods. fluids*, **7**, 1211–1228 (1987).
23. J. Kautsky and N. K. Nichols, 'Equidistributing meshes with constraints', *SIAM J. Sci. Stat. Comput.*, **1**, 499–511 (1980).
24. D. Ding and P. L.-F. Liu, 'An operator-splitting algorithm for two-dimensional convection–dispersion–reaction problems', *Int. j. numer. methods eng.*, **28**, 1023–1040 (1989).